PRELIMINARY RESULTS OF THE SURFACE RADIATION BALANCE OVER THE TROPICAL ATLANTIC OCEAN

Sarasvati A. Bacellar[1], Amauri P. de Oliveira[1], Jacyra Soares[1] and Jacques Servain[2]

Abstract: In this work the diurnal evolution of radiation balance at the surface of the Atlantic Ocean is described and analyzed. This analyses is based on observation carried out on board of the Brazilian Navy Ship *Comte Manhães*, using a net radiometer set up at 6 m above the surface. The observations are part of the observational campaign of the FluTuA Project ("Fluxos Turbulentos sobre o Atlântico"), during May 15 and 23 of 2002, between Natal, RN (6°S 35.2°W) and the São Pedro and São Paulo Archipelago (1°N 29.3°W). The solar radiation data allowed estimate the surface albedo and broadband atmospheric transmissivity. The surface emissivity was estimated from the long wave radiation surface emission and surface water temperature. During the second half of the experiment the observed albedo showed a diurnal evolution similar to the Fresnel albedo. The average surface emissivity was around 0.97. The time evolution of net radiation estimated from calibrated albedo, atmospheric transmissivity and surface emissivity agreed well with the observations indicating that the parameters are representative of the radiometric properties of the air-sea interface in the region of the Tropical Atlantic Ocean, between Natal and São Pedro and São Paulo Archipelago.

Key words: Radiation balance, and São Pedro and São Paulo Archipelago, air-sea interaction, Equatorial Atlantic Ocean and FluTuA.

Resumo: Este trabalho descreve e analisa a evolução diurna do balanço de radiação na superfície do Oceano Atlântico. A análise é baseada nas observações realizadas a bordo do Navio da Marinha do Brasil (*Comte. Manhães*), usando um radiômetro líquido a 6 m acima da superfície do oceano. Essas observações são parte da campanha observacional do Projeto FluTuA (Fluxos Turbulentos sobre o Atlântico), realizadas entre 15 e 23 de maio de 2002, entre Natal (6^0S, 35.2^0W) e o Arquipélago de São Pedro e São Paulo (1^0N, 29.3^0W). Os dados de radiação solar permitiram estimar o albedo da superfície e a transmissividade atmosférica integrada. A emissividade da superfície foi estimada da radiação de onda longa emitida pela superfície e da temperatura da superfície da água. Durante a segunda metade do experimento o albedo observado mostrou uma evolução diurna similar à do albedo de Fresnel. A emissividade média da superfície encontrada foi de cerca de 0.97. A evolução temporal da radiação liquida foi estimada usando o albedo calibrado, a emissividade da atmosfera e a emissividade da superfície concordou bem com as observações, indicando que os parâmetros obtidos são representativos das propriedades radiométricas da

[1] Department of Atmospheric Sciences, Institute of Astronomy, Geophysics and Atmospheric Sciences, University of São Paulo. Rua do Matão, 1226, São Paulo, 05508-900, SP, Brazil.

[2] FUNCEME, Av. Rui Barbosa, 1246, Aldeota, Fortaleza, 60115-221, CE, Brazil. (servain@funceme.br)

interface ar-mar na região do oceano Atlântico tropical, entre Natal e o Arquipélago de São Pedro e São Paulo.

Palavras-chave: Balanço de radiação, Arquipélago de São Pedro e São Paulo, Interação ar-mar, Oceano Atlântico tropical e FluTuA.

INTRODUCTION

The climate change issues have brought up attention to the scarcity of information about the short-term variation of ocean-atmosphere interactions. Discrepancies between climate models are known worldwide and are particularly important over the tropical and subtropical regions of the Atlantic Ocean in the Southern Hemisphere. Climate models diverge about the intensity of the heat, moisture and momentum fluxes between atmosphere and ocean (Wainer *et al*., 2003). Observations in the area are not available with the time and space resolution required. Very few observational works have been carried out in the Southern Atlantic Ocean (Dourado and Oliveira, 2001).

The present work is a description of the observations carried out on May 15-23, 2002, as part of the FluTuA Program (Bacellar, 2003; Soares *et al.* 2001). These observations were carried out on board of the Brazilian Navy Ship (Comte. Manhães) between Natal (6^0S, 35.2^0W) and São Pedro and São Paulo Archipelago (1^0N, 29.3^0W), previously known as penedos (Figure 1).

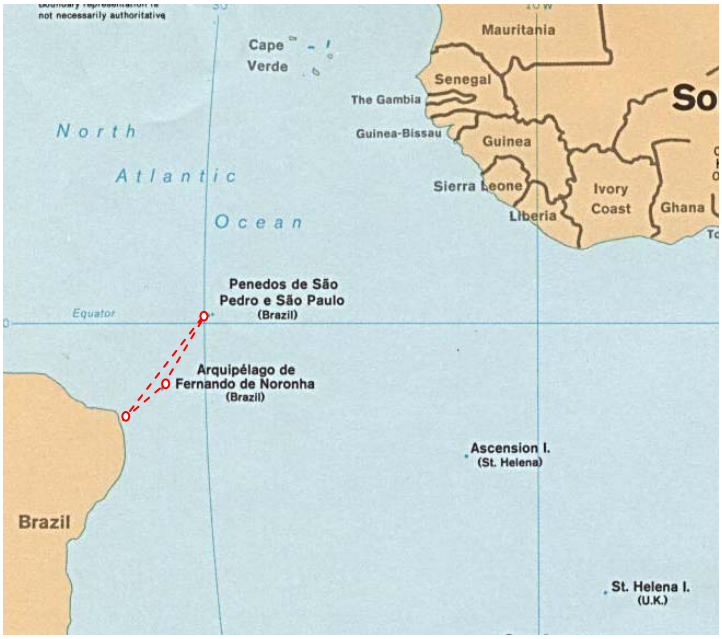

Figure 1: Geographic position of the São Pedro e São Paulo Archipelago. Trajectory described by the Manhães during the observational campaign carried out between May 15 and 23, 2002, is indicated by dashed line.

The main objective of this work is to describe the radiometric properties of the atmosphere and the ocean in the Atlantic Tropical, using the observations carried out during the expedition to SPSP Archipelago.

OBSERVATIONS

The observations were carried out on board of the Brazilian Navy ship Manhães (Figure 2). The ship was set up with wind velocity sensors, air temperature and relative humidity sensors, radiation sensor and water temperature sensor. The characteristic of each sensor is described in Table 1. The sensors were connected to the data acquisition system Datalogger 21X, manufactured by Campbell Inc. The sampling rate was set equal to 0.2 Hz and 5-minute average was calculated for all variables.

Sensor	Manufacturer	Accuracy
Net Radiometer, model CNR 1	Kipp and Zonen	2.5%
Anemometer Gill Propeller, model 27106	R.M. Yong	1%
Temperature and relative humidity model HMP45C	Vaisala	0.1ºC and 2 %
Water temperature, Vaisala, model 107	Vaisala	± 0.1 ºC

Table 1: Sensor characteristics.

The net radiation sensor was set up in the up front of the vessel, about 1 meter far from the ship, and 6 meters above the sea surface. The air temperature and relative humidity sensors were set up at the upper level of the ship, near the wind sensors, at 11 meters above the sea surface. Two anemometers were set up in the boom located at the upper level of the ship, also 11 m above the sea surface. The anemometers were oriented in the direction parallel and perpendicular to the ship (Figure 2).

The position and trajectory of the ship were obtained from an onboard GPS system (Figure 3). This information was also used to estimate the ship velocity and orientation. The ship orientation corresponds to the angle formed between the ship and east-west direction.

The wind velocity and direction were evaluated using the wind velocity measured on board of the ship and the ship velocity and direction evaluated from the GPS information.

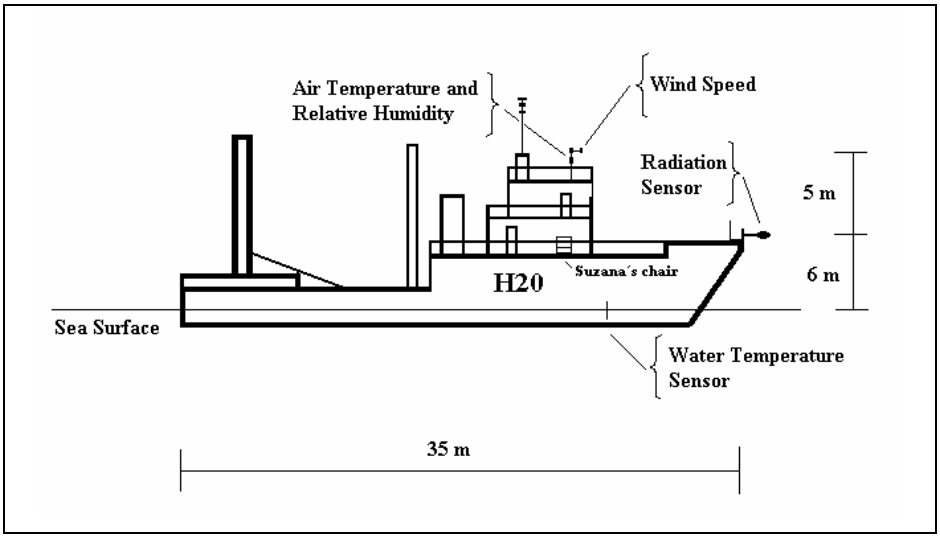

Figure 2: Schematic representation of the ship used to carry out the measurements over the Atlantic Ocean. The ship, called *Manhães*, is a military vessel used by the Brazilian Navy to launch buoys in the ocean.

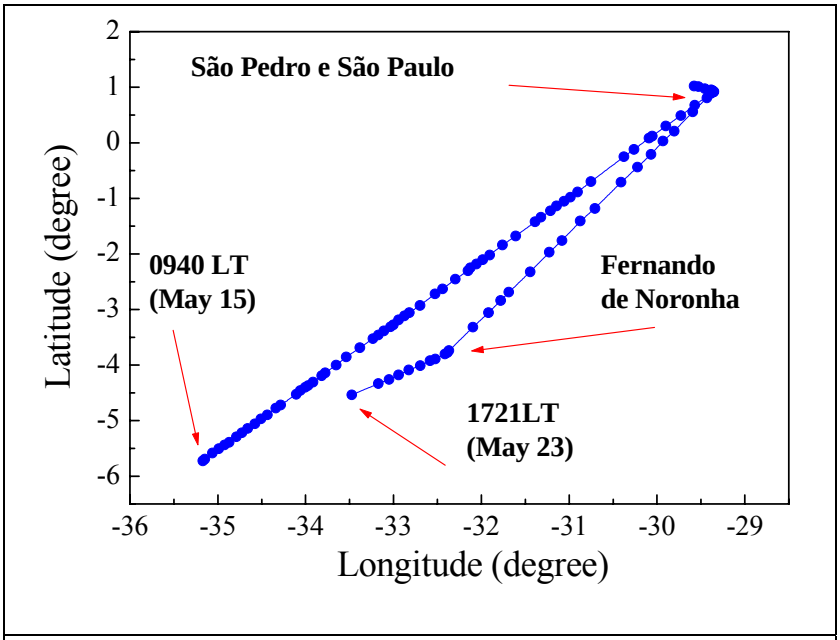

Figure 3: Trajectory described by the Manhães during the observational campaign carried out between May 15 and 23, 2002.

RESULTS

In this work the time evolution of all measured variables are reported in terms of the local time in Natal, which corresponds to the Brazilian standard time. The time changes were necessary

because the trajectory described by the ship during the field campaign covered different longitudes and the sun trajectory was evaluated taking the longitude variation into account. The time adjustment was evaluated using the time equation:

$$t_A = t_P + C_\lambda/60 + (12\,E_T)/\pi \quad (1)$$

where t_A is the local apparent time, t_P is the local time, C_λ is the correction for deviation from standard longitude and E_T is the time equation.

The longitude correction is given by:

$$C_\lambda = 4\cdot(\lambda - \lambda_P) \quad (2)$$

where λ_P is the standard longitude, in the experiment $\lambda_P = 45^0$ and λ is the longitude of the measurements. The expression above corresponds to a correction of 4 minutes for each degree of deviation from the standard longitude, positive towards west of λ_P

The incoming solar radiation at the surface $OC\downarrow_0$ was given by:

$$OC\downarrow_0 = OC\downarrow_T\ \Gamma \quad (3)$$

where Γ is the "broadband transmissivity" of the atmosphere and $OC\downarrow_T$ is the solar radiation at the top of the atmosphere estimated from:

$$OC\downarrow_T = -I_0 \cos Z \quad (4)$$

where I_0 is the solar constant given by:

$$I_0 = (\overline{D}/D)^2 S_0 \quad (5)$$

where $\overline{D}$ is the average distance between the Sun and the Earth, D is the actual Sun-Earth distance, S_0 is the average solar constant assumed equal to 1366 W m^{-2} (Frölich and Lean, 1998) and Z is the solar zenithal angle calculated from:

$$\cos Z = \text{sen}\,\phi.\,\text{sen}\,\delta + \cos\phi.\cos\delta\cos h \quad (6)$$

where, δ is the sun declination, ϕ is the latitude and h is the hourly angle.

The solar hour angle was evaluated from:

$$h = (t_A - 12)\cdot 15 \quad (7)$$

The Sun-Earth distance, solar declination and the time equation are evaluated from the expression:

$$F(\eta) = a_0 + a_1\cos\eta + a_2\sin\eta + a_3\cos 2\eta + a_4\sin 2\eta \quad (8)$$

where the constants are indicated in Table 2 and $\eta = 2\pi d^*/365$ is calculated in terms of year day (d = 0 January first and 364 for December 31).

Constant	Solar declination (δ)	Sun-Earth distance ($\bar{D}/D$)	Time equation (E_T)
a_0	0.006918	1.000110	0.000075
a_1	-0.399912	0.034221	0.001868
a_2	0.070257	0.001280	-0.032077
a_3	-0.006758	0.000719	-0.014615
a_4	0.000908	0.000077	-0.040890

Table 2: Polynomial coefficients used to estimate Sun-Earth distance, solar declination and time equation (Iqbal, 1983).

The "net sky" transmissivity (Stull, 1988, page 257) can estimated from the following expression:

$$\Gamma = (a_\Gamma + b_\Gamma \cos Z)(1 - a_{NA}\sigma_{NA})(1 - a_{NM}\sigma_{NM})(1 - a_{NB}\sigma_{NB}) \quad (9)$$

where a_Γ and b_Γ are constants that takes into consideration the clear sky depletion, a_{NA}, a_{NM}, a_{NB} are constants that takes into consideration the attenuation caused by a fraction σ_{NA} of the sky covered by high clouds, σ_{NM} of median and σ_{NB} of low clouds, respectively on the direction beam.

The block-average transmissivity, considering the ratio between *observed* global radiation at the surface and the *estimated* incoming solar radiation at the top of the atmosphere, is indicated in Figure 4. The vertical bars are small in comparison with the variation of transmissivity with the zenith angle indicating that this variation is a robust feature. The interpolated curve (Γ_2) through the averaged values is also indicated in Figure 4. The coefficient is smaller than the proposed by Stull (1988).

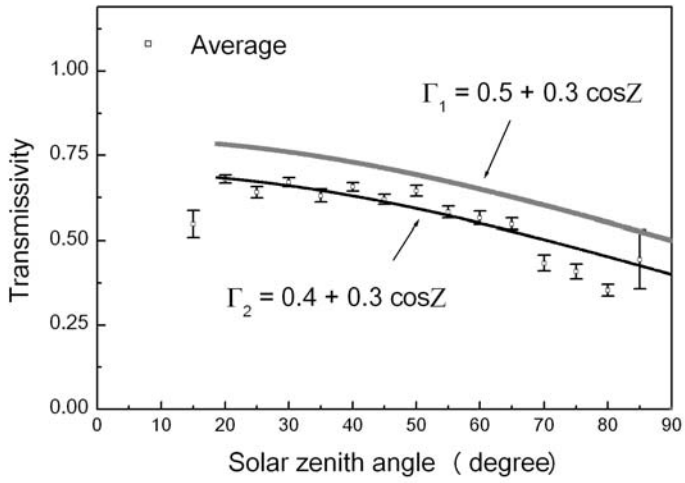

Figure 4: Average atmospheric transmissivity as function of the solar zenithal angle. The vertical bars correspond to the statistical error. Based on observations carried out during the whole campaign. Continuous lines correspond to model estimates.

Figure 5 displays the net sky atmospheric transmissivity observed (evaluated as the ratio between the observed global shortwave radiation and the solar radiation at the top of the atmosphere) and estimated by expression (9) using coefficients set derived from observed row and block-averaged transmissivity Γ_1 and Γ_2 in Table 3.

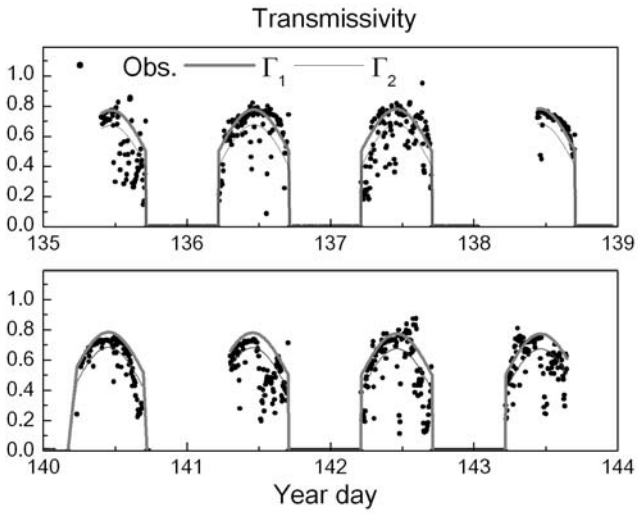

Figure 5: Atmospheric "net sky" transmissivity as a function of time. The curve Γ_1 was interpolated through the row data and curve Γ_2 was interpolated through the block-averaged transmissivity.

Source	a_r	b_r
Stull (1988)	0.6	0.2
Interpolated through row transmissivity values (Γ_1).	0.5	0.3
Interpolated through block-average transmissivity values (Γ_2).	0.4	0.3

Table 3: Coefficients for transmissivity of the atmosphere.

Figure 6 shows the solar radiation at the top of the atmosphere (estimated by expression (4)) and the observed and estimated (by expression (3)) incoming shortwave radiations at the surface. It is interesting to notice that there is a clear matching between observed and estimated global solar radiation indicating that the expression for "net sky" transmissivity is performing well.

The outgoing solar radiation from the surface was estimated from:

$$OC\uparrow_0 = -\alpha\, OC\downarrow_0 \qquad (10)$$

where α is the surface albedo.

The surface albedo is a function of transmissitivy (cloud cover), zenith angle and the state of the ocean surface (wind speed). Payne (1972) found that values of transmissivity bellow 0.1 the albedo does not depend on the solar zenith angle. On the other hand, for transmissivity between 0.60 and 0.65 the albedo show very well defined variation with solar zenith angle.

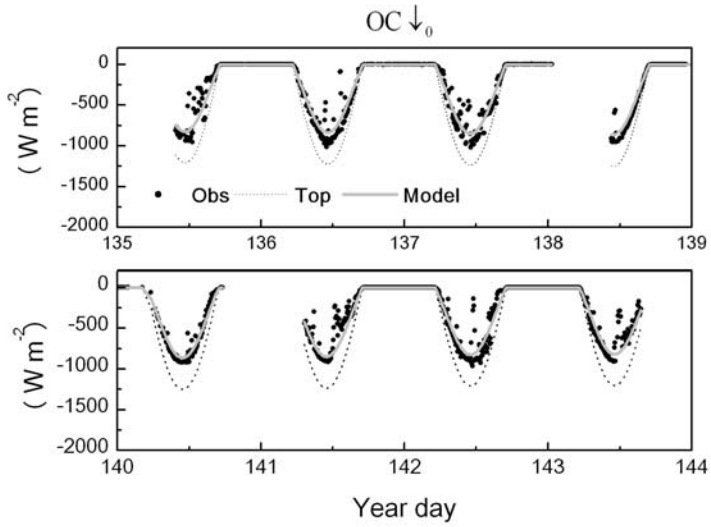

Figure 6: Observed (solid circle) and estimated (continuous gray) incoming shortwave radiations. The solar radiation at the atmospheric top is displayed in dash line.

The surface albedo can be estimated from the following expression:

$$\alpha = 0{,}50\left[\frac{\sin^2(Z-r)}{\sin^2(Z+r)}+\frac{\tan^2(Z-r)}{\tan^2(Z+r)}\right] \tag{11}$$

where r is the refraction angle of light in the water given by:

$$r = \arcsin\left[\frac{\sin Z}{n}\right] \tag{12}$$

where **n** is the seawater refraction index equal to 1.33 (Cogley, 1979).

Figure 7 shows the average surface albedo as a function of solar zenithal angle, calculated from the solar radiation observations (ratio of outgoing to incoming shortwave radiations). The average albedo for the lower zenith angles is about 0.06. This value is compatible with the albedo value found by Payne (1972), for conditions of light winds and relatively smooth seas, however it disagrees with the predicted values from Fresnel expression using coefficients for tropical latitudes (Cogley, 1979).

Considering the diurnal evolution of the albedo observed during the field campaign (Figure 8) it is observed that the discrepancy is more pronounced in the days 135 –139 when the ship was going towards SPSP Archipelago. The albedo in days 140-143 follows Fresnel. Therefore the discrepancies found in Figure 8 are caused by larger amplitude of the observed albedo during the trip to SPSP Archipelago. The possible explanation for these discrepancies is that during the trip to SPSP Archipelago the ship was facing the northern hemisphere (Figure 2) and reflecting the solar radiation increasing the albedo. In the trip from SPSP the ship was facing the southern hemisphere and the reflection caused by the ship was not significant.

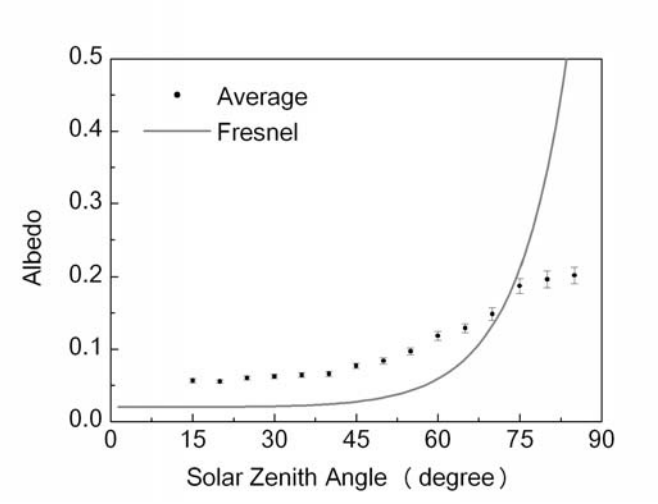

Figure 7: Average surface albedo as function of the solar zenithal angle. The vertical bars correspond to the statistical error. Based on observations carried out during the whole campaign.

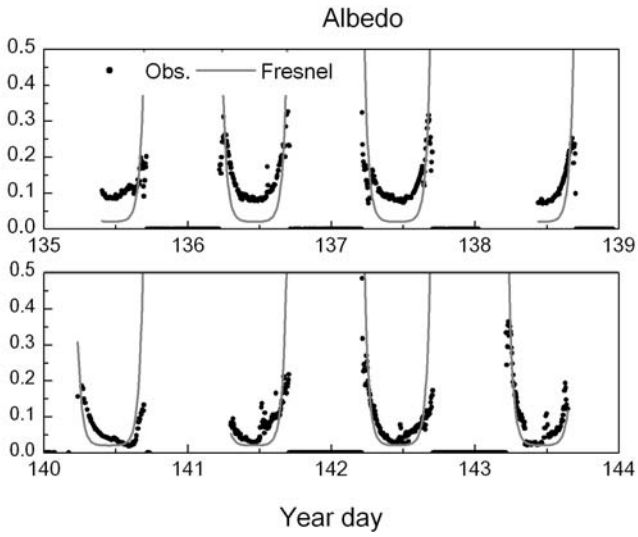

Figure 8: Albedo at the surface as function of the time.

The effect caused by the ship reflection can be identified considering the dependence between albedo and transmissivity. According to Payne, for large values of transmissivity the sea surface albedo behaves like Fresnel varying with solar elevation. In order to compare with previous studies the albedo in figures 9 and 10 are described and analyzed in terms of the sun elevation angle instead of the solar zenith angle. In both periods the albedo behavior as predicted by Fresnel (Figure 9a). For low transmissivity conditions (cloudy skies) the albedo does not depend of the position of the sun (Figure 9b). The dashed line in Figure 9 indicates the value of the albedo found by Payne for

totally cloudy conditions. During experiment reported here the albedo respond to the presence of the clouds.

Figures 10a-b shown albedo as a function of transmissivity for two values of sun elevation: 10 and 70 degrees. These values of sun elevations were estimated considering the average albedo for sun elevations between 5 and 10 degrees and 65 and 75 degrees respectively. According to these figures is possible to conclude that observations carried during FluTuA follow the Payne prediction quite well during the return leg (Figure 3), when the ship was facing the southern hemisphere (141-143). During the trip to SPSP Archipelago (Yeardays 135-139) the discrepancies are larger for sun elevation of 70 degrees as consequence of the ship reflections effects (Figure 10b).

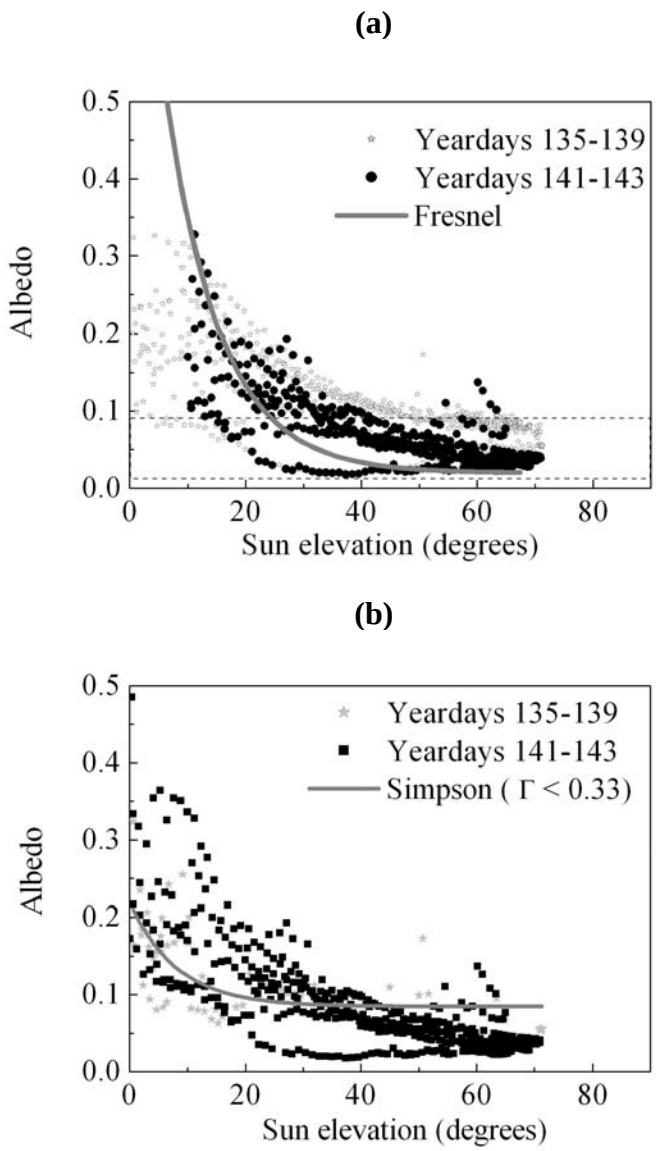

Figure 9:Albedo as a function of the sun elevation considering (a) all values of transmissivity; (b) only transmissivity < 0.30. During yeardays 135-139 the ship was facing the Northern Hemisphere. During yeardays 141-143 the ship was facing the Southern Hemisphere. Dashed line corresponds the albedo for cloudy conditions proposed by Payne (1979).

The estimated (by expressions 10-12) and observed outgoing shortwave radiations are in Figure 11. As it was discussed before the behavior of the shortwave radiation reflected by the surface of the ocean agrees with the model only during the period of observation when the ship was coming from SPSP Archipelago. The large discrepancy observed in day 140 is due to the fact that the ship was not moving in this day. This day was removed from the analysis carried out for albedo and displayed in Figs. (9)-(10).

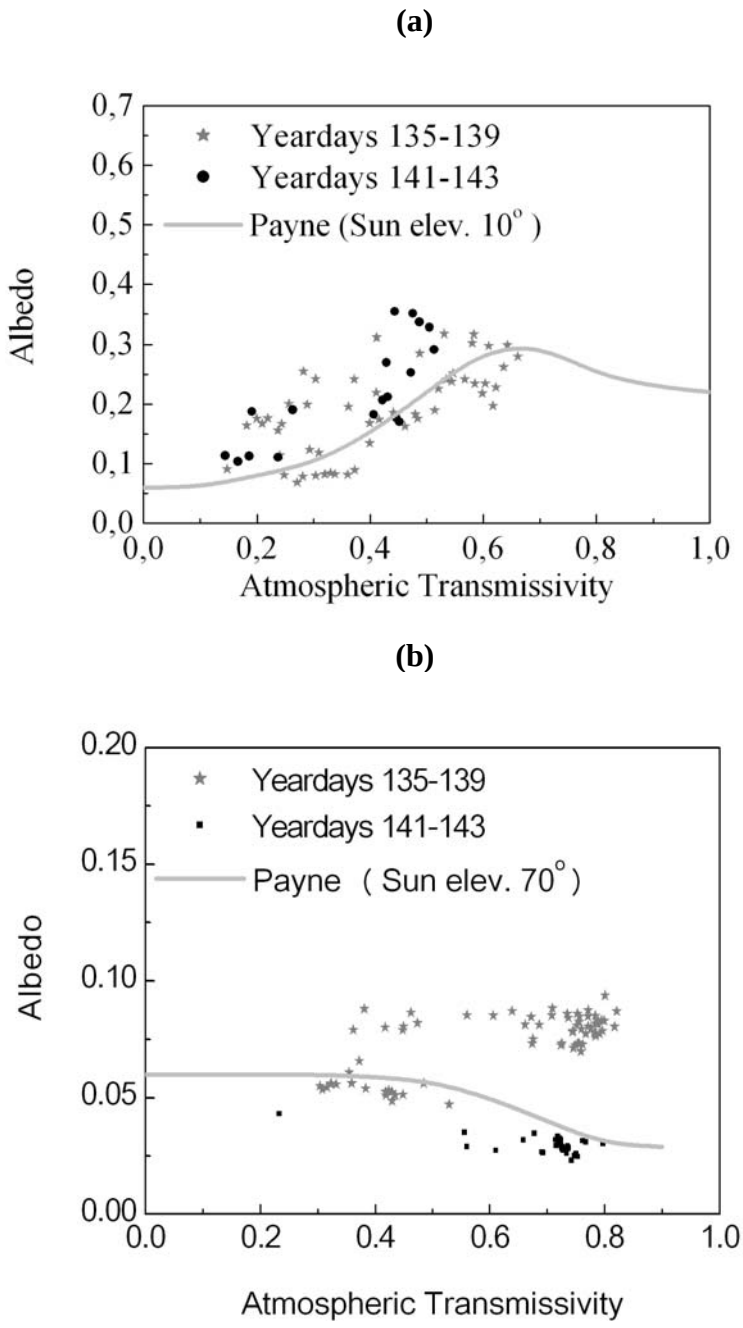

Figure 10: Albedo as a function of the atmospheric transmissivity for average sun elevation of (a) 10 degrees and (b) 70 degrees. Continuous line corresponds to Payne (1979).

The estimated (by expressions 10-12) and observed outgoing shortwave radiations are in Figure 11. As it was discussed before the behavior of the shortwave radiation reflected by the surface of the ocean agrees with the model only during the period of observation when the ship was coming from SPSP Archipelago. The large discrepancy observed in day 140 is due to the fact that the ship was not moving in this day. This day was removed from the analysis carried out for albedo and displayed in Figs. (9)-(10).

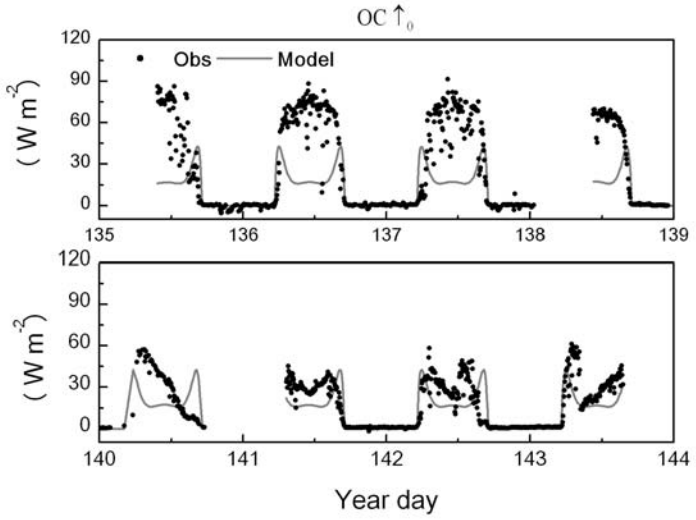

Figure 11: Observed (black solid circle) and estimated (continuous light gray line) outgoing shortwave radiations.

The outgoing longwave radiation corresponds to the emission from the surface, from the atmosphere and part of the ship located beneath the sensor level (6m). In Figure 12 the $OL\uparrow_0$ corrected by the solar effect (explained below) is indicated as a function of the time during the entire experiment. The longwave radiation emitted by the surface $OL\uparrow_0$ was calculated from the following expression:

$$OL\uparrow_0 = \varepsilon_o \sigma T_S^4 \qquad (13)$$

where ε_o is the surface emissivity, σ is the Stefan-Boltzman constant and T_S is the surface temperature.

Considering the fact that during the expedition the surface temperature did not show the diurnal cycle (Figure 13) the discrepancies found, mainly in the second period of observation, are due to the solar effects on the pyrgeometer performance discussed bellow.

The longwave radiation emitted by the atmosphere, $OL\downarrow_0$, was estimated from the following expression:

$$OL\downarrow_0 = -\left(a + b\sqrt{e_A}\right)\sigma T_A^4 \qquad (14)$$

where $\mathbf{e_A}$ is the value of vapor pressure in mb at screen level (1.5 m); **a** and **b** were set equal to 0.52 and 0.064, respectively and $\mathbf{T_A}$ is the temperature at screen level (1.5 m).

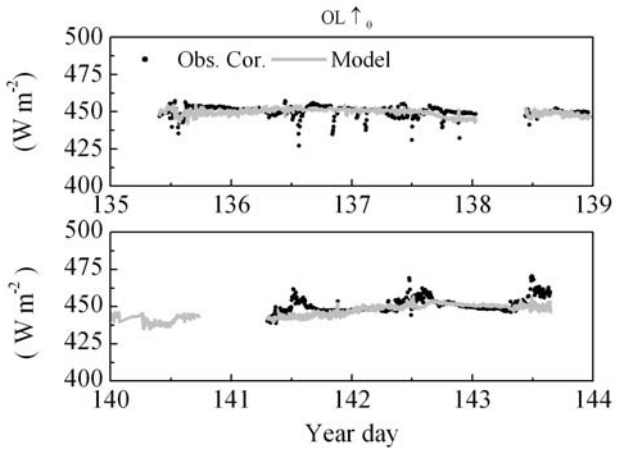

Figure 12: Observed corrected (black solid circle) and model (continuous light gray line) longwave radiation emitted by the surface of the ocean.

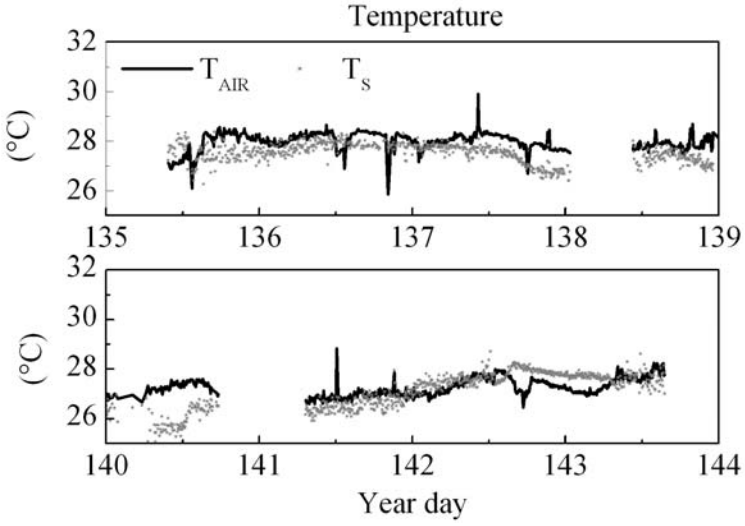

Figure 13: Air temperature observed at 11 m (continuous) and surface temperature (dotted).

Expression (14) was proposed by Brunt and is valid for clear days. Here this expression was used to estimate the downward emission from the atmosphere during the entire period, regardless the presence of clouds by using the air temperature measured on board of ship at 11 m above the sea level (Figure 14). The vapor pressure used in this expression was calculated from the observed relative humidity of the air at 11 m and considering the atmospheric pressure constant and equal to 1010 mb. The estimated atmospheric emission was systematically larger than the observed one at 6 m. In average the discrepancy is 12.5 W m^{-2}, about 3 % of the average value of the atmospheric emission.

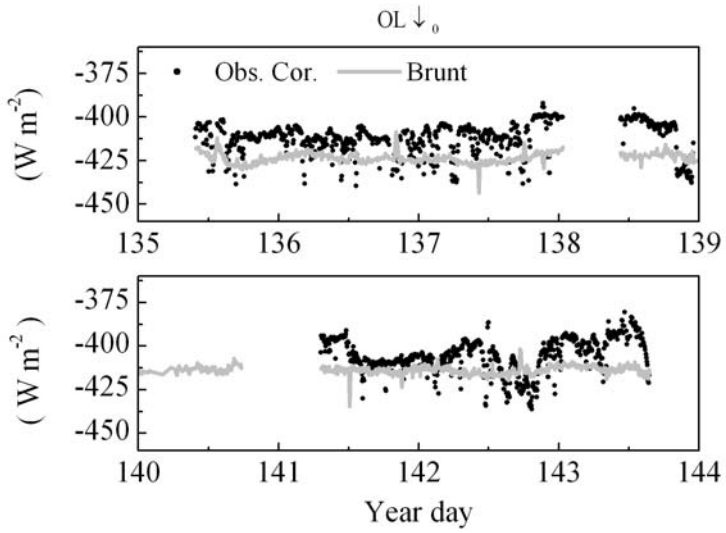

Figure 14: Observed corrected (black solid circle) and Brunt (continuous light gray line) longwave radiation emitted by the atmosphere.

The solar heating effects on the performance of the longwave radiation sensor were corrected using the following expression (Pérez and Alados-Arboledas, 1999):

$$OL_{Cor} = OL_{Obs} - 0.060 \frac{OC\downarrow_0}{\sqrt{\left|\vec{V}_{AN}\right| + 1}} \qquad (15)$$

where $\left|\vec{V}_{AN}\right| = \sqrt{u_{AN}^2 + v_{AN}^2}$ is the absolute value of the wind speed with respect to the ship, OL_{Obs} correspond to the observed value of the longwave radiation at the surface. The wind speed with respect to the ship is indicated in Figure 15. There one can see that wind was always blowing from East. The only periods when the wind was blowing form west the ship was not moving and the orientation of the ship was not available, therefore direction of the wind is not right, only the intensity.

The Perez and Alado-Arboledas expression was modified to take into account the fact that the radiometer used here (Kipp-Zonen) has a flat dome and original expression was developed for radiometer with a hemispherical dome (PIR pyrgeometer manufactured by Eppley Lab.). The value proposed by Pérez and Alados-Arboledas (1999) is 0.091, which is larger then 0.060 used here.

The larger discrepancies in the corrected values of long wave emission it was observed in the second period and it is due to the fact that the wind speed with respect to the sensor was smaller in this period because the ship was moving in the same direction of the trade winds (Figure 15).

The corrected values of surface long wave emission were used to estimate the emissivity of the surface the following expression:

$$\varepsilon_o = \frac{\left[OL\uparrow_0\right]_{Cor}}{\sigma T_S^{\,4}} \tag{16}$$

where Ts is the surface temperature measured with thermistor dropped in the water (Figure 14). It is interesting to observe that during most of the trip the surface temperature was about 2 degrees colder than the air at 11 m.

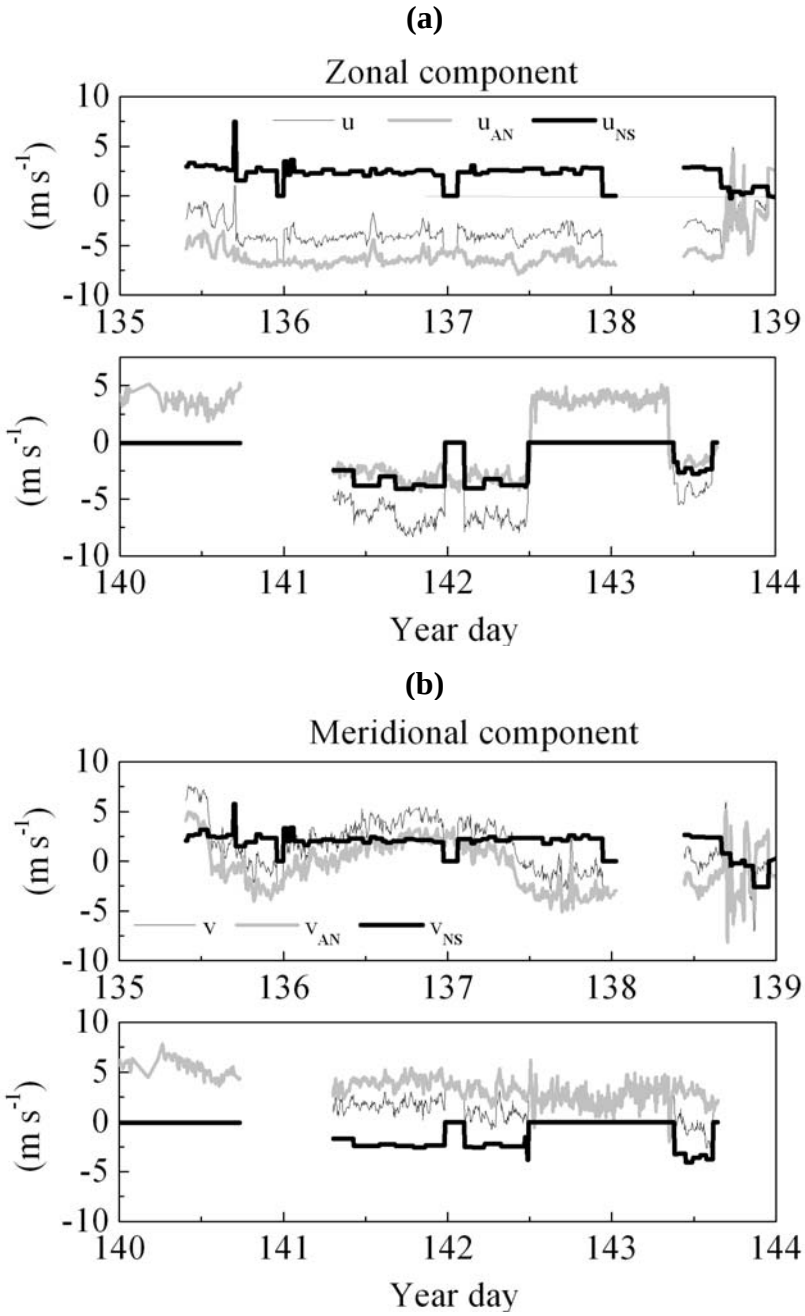

Figure 15: Zonal and meridional components of the wind velocity with respect to the surface (u, v), the ship (u_{AN},v_{AN}) and ship velocity components (u_{NS},v_{NS}).

The frequency of the surface emissivity values is displayed in Figure 16. There one sees that the most probable value of surface emissivity is 0.97. This value is consistent with other observations for ocean (Bhat *et al.*, 2003).

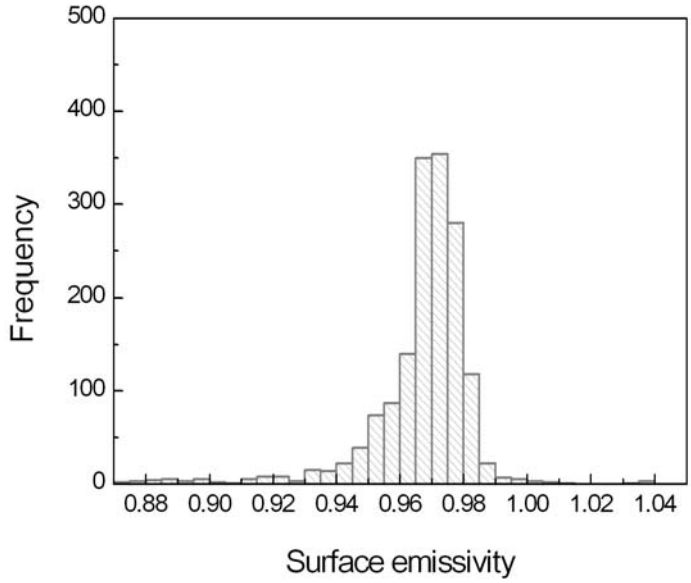

Figure 16: Frequency of surface emissivity values. The maximum frequency is equal to 0.97.

The net radiation, Rn_0, at the ocean surface was evaluated considering the shortwave and longwave atmospheric components at the air-sea interface:

$$Rn_0 = OC\uparrow_0 + OC\downarrow_0 + OL\uparrow_0 + OL\downarrow_0 \qquad (17)$$

where the short wave radiation components $OC\downarrow_0$ and $OC\uparrow_0$ were evaluated from expression (3) and (10). In the expression (3) it was used the transmissivity expression Γ_1 and for expression (10) it was used the albedo expression proposed by expression (11). The long wave radiation components $OL\uparrow_0$ and $OL\downarrow_0$ were estimated from expression (13) and (14). In the expression (13) it was used the estimated emissivity (0.97).

In the Figure 17 the Rn_o modeled is compared with the observed values. One sees that the modeled values match the observation well.

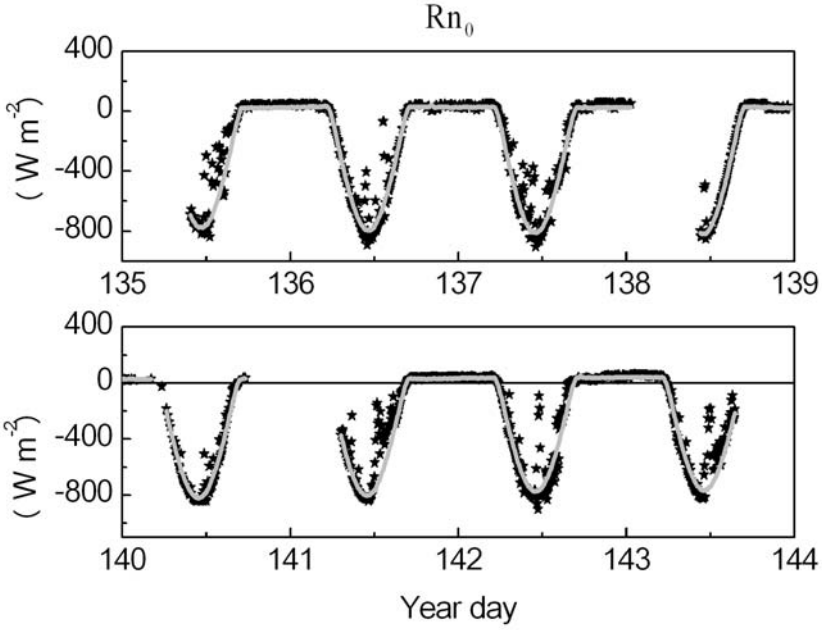

Figure 17: Observed (stars) and estimated (continuous gray line) net radiation.

CONCLUSION

The observational campaign carried out on May 15-24, 2002, as part of the FluTuA Program, is described here. During 9 days, 5 minute averaged measurements of (a) solar radiation fluxes (incoming and outcoming) and longwave radiation fluxes (atmospheric and surface emission), at 6 m above the sea level; (b) air temperature, relative humidity and horizontal wind components, at 11 m and (c) sea surface temperature were gathered continuously.

These observations were carried out on board of the Brazilian Navy Ship (*Comte. Manhães*), between Natal (6^0S, 35.2^0W) and Archipelago de São Pedro e São Paulo (1^0N, 29.3^0W).

The averaged transmissivity of the atmosphere follows the expression: $\Gamma = (0.4 + 0.3\cos Z)$. This expression was obtained fitting this curve through the observed block averaged transmissivity, however it underestimates the diurnal evolution of the atmospheric transmissivity because it includes the effects caused by clouds. In fact, the best matching with observed atmospheric transmissivity was obtained from: $\Gamma = (0.5 + 0.3\cos Z)$.

The observed albedo shows a very pronounced diurnal cycle, varying from 0.05 around noontime to infinity at the end of the day. In the first part of the observed period spurious reflection from the vessel increased the albedo. The albedo varies with sun elevation angle and atmospheric transmissivity according to the observation carried by Payne (1979) and Simpson (1980). The observed albedo follows the Fresnel expression during the second part of the experiment. This

indicates that Fresnel expression can be used to estimate the albedo over the Atlantic Ocean tropical.

The Brunt expression using the air temperature and water vapor pressure observed at 11 meters above the surface overestimated the values of atmospheric emission in about 3 % in average. This is a fairly acceptable result considering that presence of clouds and effects caused by emission from the vessel.

Emissivity of the surface was estimated from observed long wave emission from the surface and blackbody emission obtained from the observed sea surface temperature. The most probable value is 0.97, matches with literature.

The time evolution of net radiation estimated from calibrated albedo, atmospheric transmissivity and surface emissivity agrees well with the observation indicating that these parameter are representative of the radiometric property of the atmosphere-ocean interface in the region of Equatorial Atlantic, between the Brazil and the São Pedro and São Paulo Archipelago.

Acknowledgments. The authors acknowledge the financial support provided by CNPq, Fapesp, USP/COFECUB (UC 27/96) and CNPq/SCI (910072/00-0) by the Pró Arquipelago Program. We thank the Brazilian Navy, in special the chief officer Jean Félix de Oliveira and his helpful crew. We also thank Susanna Sichel for her valuable service as an assistant.

REFERENCES

Bacellar, S.A., 2003: Balanço de radiação na superficie do Oceano Atlântico (2003): 100 pp. (http://www.iag.usp.br/meteo/labmicro/Sara_REL_FluTuA_2003.PDF).

Bhat, G.S., Thomas, M.A., Raju, J.V.S. and Chandrasekhara, C.P., 2003: Surface Characteristics observed near the central tropical indian ocean during INDOEX IFP99. *Bound.-Layer Meteorol.,* **106**, 263-281.

Cogley, J.G., 1979: The albedo of water as a function of latitude. *Monthly Weather Review*, **107**, 775-781.

Iqbal, M., 1983: *An Introduction to Solar Radiation*. Academic Press, 390 pp.

Pérez, M. and Alados-Arboledas, L., 1999: Effets of Natural Ventilaion and Solar Radiation on the Performance of Pyrgeometers, *Journal of Atmospheric and Oceanic Technology*, **16**, 174-80.

Dourado, M., and Oliveira, A. P., 2001: Observational description of the atmospheric and oceanic boundary layers over the Atlantic Ocean. *Revista Brasileira de Oceanografia,* **49**, 49-64.

Frölich, C. and Lean, J., 1998: The sun's total irradiance: Cycles and trends in the past two decades and associated climate change uncertainties. *Geophys. Res. Let*. **25**, 4377-4380.

Payne, R.E., 1972: Albedo of the sea surface. *J. Atmos. Sci.,* **29**, 959-970.

Simpson, J.J. and Paulson, C.A., 1979: Mid-ocean observations of atmospheric radiation. *Quart. J. R. Met. Soc.*, **105**, 487-502.

Soares, J., Oliveira, A. P., Wainer, I., Servain, J., 2001: Turbulent fluxes over the tropical Atlantic Ocean. *Proceedings of the WCRP/SCOR Workshop Intercomparison and Validation of Ocean-Atmosphere Flux Field*, 21-24 May 2001, Washington, DC, EUA, 334-337.

Stull, R.B., 1988: An Introduction to Boundary Layer Meteorology. Dordrecht: Kluwer, 666p.

Wainer, I., Taschetto, A.; Soares, J.; Oliveira, A.P., Otto-Bliesner, B. and Brady, E., 2003: Intercomparison of heat fluxes in the South Atlantic. Part 1: The Seasonal Cycle. *Journal of Climate*, **16(4),** 706-714.